SCATTEROMETRY DATA SETS: HIGH QUALITY WINDS OVER WATER

Mark A. Bourassa*, David M. Legler and James J. O'Brien, Center for Ocean-Atmospheric Prediction Studies (COAPS), Florida State University, USA

1. INTRODUCTION

In the late 1990s microwave scatterometry is finally catching up to other radiometric instruments of the SeaSat era: altimeters (ocean height and wave height), radiometers (temperatures and humidity), and scatterometers (wind speed and direction), all designed to provide the previously unattainable quantity and quality of data regarding variability of the ocean and adjoining atmospheric boundary-layer (Katsaros and Brown, 1991). Europeans have been working with two successive scatterometers beginning in 1991. These scatterometers on the European Remote Sensing Satellite Systems (ERS-1 and ERS-2) provided the first scatterometer data that could be used for climatological studies. Operational constraints have prevented continuous scatterometer observations over water; however, the scatterometer was usually operating away from land and ice.

The Japanese satellite, ADEOS, which was launched in August 1996, had the first dedicated microwave scatterometer since SeaSat: the NASA Scatterometer (NSCAT). This scatterometer determined wind speed and direction over 90 per cent of the ice-free global water surface in two days with 25-km in-swath resolution. It functioned until a catastrophic failure of the satellite platform on 29 June 1997. Despite this loss, the unprecedented coverage and resolution of global wind data gave light to profound impacts on oceanographic and meteorological applications.

The unprecedented accuracy and coverage of NSCAT winds led to the rapid deployment of a new type of scatterometer (SeaWinds) to fill the void in NSCAT-like observations. SeaWinds instruments are on QuikSCAT (launched on 19 June, 1999) and ADEOS-2 (planned). SeaWinds scatterometers have approximately double the coverage of NSCAT, covering 90 per cent of the world's oceans in one day. The NSCAT and SeaWinds periods may be the only times to date when ocean modellers could not reasonably argue that errors in model output were due mainly to shortcomings in wind observations. Owing to the relatively recent development of these wind products, few researchers are aware of their nature and quality. This report describes the wealth of current products, as well as providing a brief discussion of their strengths and weaknesses.

Several types of data sets, appropriate to different applications, are publicly available. The swath winds (i.e. gridded relative to the satellite track) are available for those who need near-instantaneous winds that are not further processed (e.g. Jones *et al.*, 1999). For example, comparisons of these winds to research vessels (R/Vs) (Bourassa *et al.*, 1997) and National Data Buoy Center (NDBC) buoys (Freilich and Dunbar, 1999) have shown that these winds could be used to quality control ship and buoy observations. However, these data sets are not regularly gridded in a latitude-longitude grid, and have gaps in daily coverage. Most ocean modelling applications require winds (or stresses) to be regularly gridded in space and time, with no missing data over water. Many such gridded daily products are also available. Such products are also useful in constructing wind vector climatologies that include synoptic-scale and some mesoscale variations (e.g. Bourassa *et al.*, 1999*b*; Chelton *et al.*, 2000; Milliff *et al.*, 1999*a*). Animations of gridded products (Bourassa *et al.*, 1998, 1999*b*) have also been developed for data visualization. Animations are of great use in examining the vast quantity of scatterometer data to find features of

*Corresponding author's address: Center for Ocean-Atmospheric Prediction Studies, Florida State University, Tallahassee, Florida 32306-2840, USA; e-mail: bourassa@coaps.fsu.edu; Telephone: (850) 644-6923, FAX: (850) 644-4841

interest. They clearly show frontogenesis, cyclogenesis, and larger scale circulation patterns. These scatterometer data products will be discussed.

2. SCATTEROMETRY BACKGROUND

Scatterometers are unique among satellite remote sensors because of their ability to accurately determine wind speed and direction. Microwaves are Bragg-scattered by short water waves, which respond quickly to changes in winds. This backscatter (the fraction of transmitted energy that returns to the satellite) is a function of wind speed and wind direction. The wind direction is found by determining the angle that is most likely to match the observed backscatters. A digital filtering technique (Naderi *et al.*, 1991) is used to sample locations from multiple angles in less than five minutes. There are substantial design differences for ERS scatterometers, NSCAT, and SeaWinds (Table 1). For example, the ERS backscatter is spatially smoothed, thereby reducing the resolution to ~70 km (M.H. Freilich and D.G. Long, 1998, personal communication). On NSCAT, there were three fixed antennas on each side, allowing swaths on each side of the satellite track to be sampled by fore, mid, and aft beams. Wind speeds and directions were calculated when radar observations were available from all three of these antennas. In contrast, ERS scatterometers are sometimes forced to use observations from only two antennas (Zeccheto *et al.*, 1999). For fixed-antenna scatterometers (SeaSat, ERS-1/2 and NSCAT), the use of three or more antennas is essential for accurate determination of the wind direction (Naderi *et al.*, 1991). The beam arrangement on SeaWinds instruments is a new design, with two conically rotating beams at fixed incidence angles. This design allows a single, very wide observational swath. This scanning geometry has four substantially different angles over an area similar to the NSCAT swaths. However, near nadir and near the edges of the swath, the angles are similar, resulting in decreased accuracy in these parts of the swath. Furthermore, only one of the two beams reaches the outer 75 km of the swath. These problems are somewhat compensated by a much greater observation density. NSCAT had three or four observations within a 25 × 25 km cell, whereas SeaWinds typically has between eight and 25 observations within its 25 × 25 km cells.

The functions describing the wind direction are sinusoidal. Combining these functions to minimize the misfit usually results in multiple minima (ambiguous solutions often called ambiguities). Ideally, for fixed-antenna scatterometers, the best fit corresponds to the correct direction, the next best fit is in approximately the opposite direction, and the next two minima are in directions roughly perpendicular to the wind direction. For SeaWinds scatterometers, the solution geometry varies across the swath. The solutions are similar to fixed-antenna scatterometer solutions in the part of the swath similar to NSCAT coverage, but differ greatly near nadir and

Table 1—Scatterometer characteristics. Note that for ERS-1/2 scatterometers, the three cells closest to nadir do not meet all the desired retrieval requirements; wind vectors from these cells are often ignored.

Scatterometer	*Period in service*	*Scan characteristics*	*Swath width (km)*	*Nadir gap (km)*	*In-swath grid Spacing (km)*	*Cell size (km)*	*Scan characteristics*	*Operational frequency*
ERS-1 Scatterometer	1991/7 to 1997/5/21	one-sided (single swath)	475	NA	25 × 25	50 × 50	one-sided (single swath)	C band (5.3 GHz)
ERS-2 Scatterometer	1997/5/21 to current	one-sided (single swath)	475	NA	25 × 25	50 × 50	one-sided (single swath)	C band (5.3 GHz)
NSCAT	1996/9/15 to 1997/6/30	two-sided (double swath)	600	329	25 × 25 50 × 50	25 × 25 50 × 50	two-sided (double swath)	Ku band (13.995 GHz)
SeaWinds on QuikSCAT	~1999/7/19 to current	conical scan, one-wide swath	1900	NA	25 × 25	25 × 25	conical-scan, one wide swath	Ku band (13.995 GHz)
SeaWinds on ADEOS II	TBA	conical scan, one-wide swath	1900	NA	25 × 25	25 × 25	conical-scan, one wide swath	Ku band (13.995 GHz)
ASCAT	TBA	two-sided (double swath)	550	660	25 × 25	50 × 50	two-sided (double swath)	C-band (~5.3 GHz)

near the swath edges. The process of choosing the direction is called ambiguity selection. Noise and spatial/temporal variability can change the quality of fit and thereby cause incorrect directions (also known as aliases) to be chosen. NSCAT's ambiguity removal was further improved by using two polarizations with one antenna, whereas SeaWinds ambiguity selection is improved by greater observation density. For NSCAT and QuikSCAT winds, a median filter (applied to ambiguity selection rather than wind direction) is also used to improve ambiguity selection.

Rain influences radar returns through three processes: backscatter from rain drops, attenuation of the signal passing through the rain (Moore *et al.*, 1999), and modification of the sea surface shape by raindrop impacts (Bliven *et al.*, 1993; Sobieski and Bliven, 1995; Sobieski *et al.*, 1999). The influence of these considerations on the accuracy of winds is a function of scatterometer design. Rain has a greater influence at large incidence angles (the signal passes through more rain) and for Ku-band (NSCAT and SeaWinds) rather than C-band (ERS-1/2). Rain is not considered a serious problem for the ERS scatterometers. For NSCAT, rain contributed to substantial errors in the outer parts of the swaths; however, rain can have a substantial influence on SeaWinds observations throughout the swath. Modelling these problems is a concern of ongoing research (Weissman *et al.*, 2000). In the meantime, several rain flags are being developed. On ADEOS-2, rain-related contamination will be identified through co-located rain observations from sensors aboard the satellite.

3. SWATH DATA

Scatterometers are carried onboard polar orbiting satellites. QuikSCAT and NSCAT have been in sun synchronous orbits, with approximately 15 orbits per day. Polar orbits, in contrast to the geostationary orbits of more routinely used weather satellites, have areas of coverage that change with time. One great advantage of using polar orbits is obtaining observations at latitudes much farther from the equator than can be achieved with geostationary orbits. Polar-orbiting satellites take observations in swaths below and/or to the sides of the satellite (usually described relative to its forward motion). The ERS-1/2 scatterometer observations come from a 500 km wide swath on only one side of the satellite. NSCAT more than doubled this coverage by measuring the return signals from 600 km wide swaths on both sides of the satellite, with a 400 km wide nadir gap below the satellite (Figure 1). The spatial coverage of SeaWinds scatterometers is doubled again by filling the nadir gap and extending the far edges of the swath another 75 km. The observation rate is staggering, with the number of daily observations provided by SeaWinds approximately equal to the number of annual wind observations routinely provided by all buoys and ships available through the Global Telecommunication System (GTS) data stream.

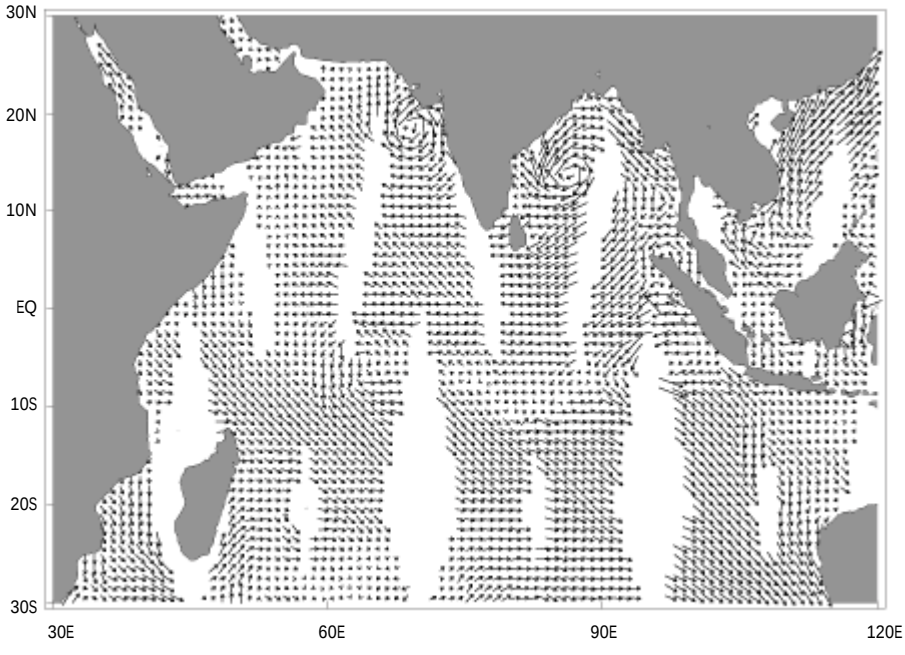

Figure 1—NSCAT observations from 26 October 1996, vector averaged in 1 × 1° bins. The single day of observations captures cyclones in the Arabian Sea and the Bay of Bengal.

Winds determined with the NSCAT-1 geophysical model function (Wentz and Smith, 1999) have been validated against a wide range of in situ and remotely-sensed winds. NSCAT and SeaWinds wind speeds have been calibrated to 10 m 'equivalent neutral wind speeds' (Liu and Tang, 1996; Verschell *et al.*, 1999), which differ from wind speed in a manner believed to be consistent with the physics to which the scatterometer responds. The differences can easily be explained with the equation for the modified log-wind profile:

$$U(z) - U_{sfc} = (u_* / k) [\ln (z/z_o) - \varphi(z, z_o, L)] \quad (1)$$

where U is the vector wind, U_{sfc} is the velocity frame of reference (the surface current), u_* is the friction velocity, k is von Karman's constant, z is the height above the local mean surface (10 m in this case), z_o is the roughness length, φ is a function of atmospheric stability, and measure of atmospheric stability is the Monin-Obukhov scale length (L). Scatterometers respond to the sea surface ($z \approx 0$), and the stability term (φ) is largely a function of z/L. Therefore, the concept is to eliminate the stability term in the height adjustment. Equivalent neutral wind speed (Cardone *et al.*, 1969; Ross *et al.*, 1985; Cardone *et al.*, 1996; Liu and Tang, 1996, Verschell *et al.*, 1999) is parametrized similarly to (1) and uses the same non-neutral values of u_* and z_o; however, the stability term (φ) is set to zero. Hence, the differences between U_{10EN} and U_{10} are stability dependent.

$$U_{10EN} - U_{10} = u_* \varphi (z, z_o, L) / k \quad (2)$$

It considers that the scatterometer probably responds to stress rather than wind speed. The kinematic stress is equal to the square of the friction velocity; therefore, the friction velocity used in the calibration of scatterometer winds should be the non-neutral value rather than the neutral value. Relatively large values of $|U_{10EN} - U_{10}|$ tend to be associated with very stable stratification. Values of $|U_{10EN} - U_{10}|$ are usually <0.5 m s^{-1} (hereafter U_{10EN} will be referred to as winds).

Studies comparing scatterometer winds to in situ observations have been made with buoys, Voluntary Observing Ships (VOSs), and R/Vs (Table 4). These studies investigate the accuracy of wind speed, wind direction (usually for correctly selected ambiguities) and vector winds (Freilich and Dunbar, 1999), as well as the fraction of correct ambiguity selection. These studies usually determined the rms difference between scatterometer and in situ winds, which provides an upper limit on uncertainty in scatterometer winds (since a substantial fraction of the differences is probably due to uncertainty in the comparison data set). The findings are summarized in Table 4.

Underestimation of NSCAT-1 model function wind speeds for $U_{10} > 20$ ms^{-1} (R. Brown and R. Foster, 1997, personal communication, Jones *et al.*, 1999), as well as biases in selection of ambiguities (Ebuchi, 1999), led to the development of the NSCAT-2 and NSCAT-2p geophysical model functions. For most applications, the differences in NSCAT-1 and NSCAT-2 winds are very small; however, for high wind speed problems these changes are systematic and could be significant. The differences between the NSCAT-2 and NSCAT-2p model functions are also small (F. Wentz and M. H. Freilich, 2000, personal communications); however, they led to improved impact in the weather model forecasts (R. Atlas, 2000, personal communication). The NSCAT-2p model function is consistent with the JPL model function (QSCAT-1) currently used for the SeaWinds scatterometer. An alternative SeaWinds model function (Ku-2000) has been developed by Remote Sensing Systems (F. Wentz and D. Smith, 2000, personal communication). The following is the first published evaluation of the NSCAT-2, QSCAT-1, and Ku-2000 model functions.

3.1 VALIDATION OF NSCAT-2 AND QSCAT-1 WINDS

The differences between scatterometer winds and the comparison data sets were often expressed in terms of rms differences (for correctly selected ambiguities) due to programmatic requirements on accuracy. When there is no uncertainty in the comparison data set, no biases in either data set (or equal biases), and no complications due to geophysical inconsistencies (e.g. space and time scales or inexact

Scatterometer	*Comparison data set(s)*		*Comparison statistics* (ms^{-1})	(deg.)	*Qualifiers*	*Model function or product*	*Reference*
ERS-1/2	Buoys	NDBC ODBS TAO	2.0 1.9 1.8	41° at 0-50 ms^{-1} 23° at 5-50 ms^{-1} 21° at 5-50 ms^{-1}* * Excludes inner 3 cells	Speeds: r, SA Directions: s, SA	JPL CMOD4-FD	Graber *et al.* (1996)
		NDBC ODBS TAO	1.6 1.8 1.8	55° at 0-50 ms^{-1} 40° at 5-50 ms^{-1} 37° at 5-50 ms^{-1}* * Excludes inner 3 cells	Speeds: r, SA Directions: s, SA	CMOD4	Graber *et al.* (1996)
		NDBC ODBS TAO	1.3 1.3 1.3	25° at 3-50 ms-1 22° at 5-50 ms^{-1} 21° at 5-50 ms^{-1}* * Excludes inner 3 cells	Speeds: r, SA Directions: s, SA	IFREMER	Graber *et al.* (1996)
		NDBC	2.5	_	c, s, SA	Operational CMOD4	Frelich (1997)
		NDBC NCEP	1.7 1.4	zonal component meridional comp.	c, r, SA	COMD4	Stoffelen (1998)
ERS-2	Ships	VOS	3.3	24	r, CA	Operational CMOD-4	Atlas *et al.* (1999)
NSCAT	Ships	Research	1.4	12 for 2-20 ms^{-1}	r, CSA	NSCAT-1	Bourassa *et al.* (1997)
		Research	<1.3	<10 for 2-20 ms^{-1}	u, CSA	NSCAT-2	This article
		VOS	2.7	21	r, CA	NSCAT-1	Atlas *et al.* (1999)
	Buoys	NDBC	1.3	30° at 3 ms^{-1} 17° at 5 ms^{-1} 14° at >10 ms^{-1}	S, CSA	NSCAT-1	Freilich and Dunbar (1999)
		NDBC	2.0	18.8	r, CA	NSCAT-1	Atlas *et al.* (1999)
		NDBC	0.6	_	c, s, SA	NSCAT-2	Freilich and Vanhoff (2000)
		TAO	1.14	33 20	r, SA r, CA	NSCAT-2	Dickenson *et al.* (2000)
		TAO	1.6 1.2 1.1 1.4 2.9	54° at 0-5 ms^{-1} 25° at 5-7.5 ms^{-1} 17° at 7.5-10 ms^{-1} 20° at 10-12.5 ms^{-1} 20° at 12.5-50 ms^{-1}	Speeds: r, SA Directions: s, SA	NSCAT-2 (25 km)	Caruso *et al.* (1999)
		WHOI	1.6 0.68 0.79 3.9	54° at 0-5 ms^{-1} 18° at 5-7.5 ms^{-1} 15° at 7.5-10 ms^{-1} 6° at 10-12.5 ms^{-1}	Speeds: r, SA Directions: s, SA	NSCAT-2 (25 km)	Caruso *et al.* (1999)
	Model	GEOS-1	2.8	22	r, CA	NSCAT-1	Atlas *et al.* (1999)
	winds	NCEP	2.0	19	r, CA	NSCAT-1	Atlas *et al.* (1999)
QuikSCAT	Ships	Research vessels	<0.45	<5° for 2-20 ms^{-1}	u, CSA	QSCAT-1	Bourassa *et al.* (2001)
		Research vessels	<0.3	<3° for 2-20 ms^{-1}	u, CSA	Ku-2000	Bourassa *et al.* (2001)

Table 4—Uncertainties in scatterometer observations. Many different assumptions (listed in the column labelled 'Qualifiers') have been used to determine these statistics: closest ambiguities (CA), correctly selected ambiguities (CSA), selected ambiguities (SA), vector wind component rather than speed (c), rms difference (r), standard deviation (s), uncertainty (u).

co-location), rms differences (and standard deviations) are essentially identical to traditional estimates of uncertainty. The scatterometer rms differences (and standard deviations) in Table 4 included contributions from the problems listed above, as well as geophysical differences due to in situ wind observations being earth relative, and the scatterometer winds being surface relative. Differences between random uncertainty and rms differences are highlighted in the comparison of ERS winds from various model functions to buoy winds (Table 4). The rms differences are substantially different for each model function; however, these differences are due more to biases than to differences in random uncertainty (Graber *et al.*, 1996). An accurate assessment of uncertainty, which is far more useful than an rms difference, requires that these additional factors be considered.

The uncertainty in the comparison data set is difficult to assess in this case since there is no absolute standard of truth for ocean winds. Techniques for estimating uncertainty in observations and comparison data sets have been developed (Stoffelen, 1998) using a third set of co-located observations. This approach uses the estimated uncertainties in the calculation of systematic gains and offsets. A similar approach, modified to consider a random component error (Freilich and Vanhoff, 2000), efficiently deals with the low wind speed problems identified by Freilich (1997). Unfortunately, these techniques require at least thousands of collocated observations from three sources. Such a large quantity of co-locations is not readily available from R/V data. An elegant alternative to these approaches is Principal Component Analysis (PCA; Pearson, 1901; Preisendorfer and Mobley, 1988), which assumes that the uncertainty in the comparison data set is equal to the uncertainty in the observations. This approach finds the variance perpendicular from a best-fit line. In the case of our comparisons between quality controlled ship observations and correctly selected ambiguities of NSCAT and SeaWinds observations, this assumption is good; otherwise a more complicated technique would be needed.

The uncertainty in the comparison data set (at the location of the satellite observation) is reduced by restricting this analysis to coincident satellite and R/V observations. For the calculation of rms differences, the central differences in observation times are less than twenty minutes (usually <30s), and the differences in locations were <25 for the NSCAT 25 km product, <50 km for the NSCAT 50 km product, and <12.5 km for SeaWinds. The co-location distance requires greater consideration, because the rms differences and estimated uncertainties are highly dependent on co-location distance. This point will be demonstrated in section 3.4 on QuikSCAT directional uncertainty.

The observations come from many ocean and atmospheric conditions (Tables 2 and 3); consequently, net biases in these findings due to location are unlikely, a specific sea state or atmospheric stability. There were 135 co-locations for the 25 km NSCAT product, 424 co-locations with SeaWinds QSCAT-1 product, and 425 co-locations with the SeaWinds Ku-2000 product. In all cases, wind speeds ranged from 2 to 20 m s^{-1}. A boundary-layer model (Bourassa *et al.*, 1999*a*) is used to adjust the R/V wind speeds to neutral equivalent winds at a height of 10 m, the height for which scatterometer winds are calibrated.

3.2 SHIP OBSERVATIONS

Wind directions from quality controlled R/V observations have proven to be the most consistently accurate source of in situ surface comparison (Table 4). True winds (i.e. speeds relative to the fixed earth and directions relative to true north) from ships that are correctly calculated (Smith *et al.*, 1999) do not suffer from either the directional shortcomings of typical buoys (in light winds or heavy seas) or the large uncertainties in VOS observations (Pierson, 1990). Preliminary

Table 2—Research vessels used in NSCAT validation.

Ship	*Location*	*Time*
RSV Aurora Australis	Southern Ocean	Sept., Nov. 1996
R/V Knorr	North Atlantic	Oct. 1996 to March 1997
R/V Thompson	North and tropical Pacific	July-Sept. 1996

Table 3—Vessels used in QuikSCAT validation.

Ship	*Location*	*Time*
R/V Atlantis	Gulf of Alaska	July, Aug. 1999
RSV Aurora Australis	Southern Ocean	July–Sept. 1999
R/V Knorr	North and Eq. Atlantic	Jan.–June 2000
R/V Melville	Tropical Pacific	July–Nov. 1999
R/V Meteor	North Atlantic	July 1999 to Aug. 2000
R/V Oceanus	North Atlantic	July–Dec. 1999, April 2000
R/V Polarstern	North Atlantic	July 1999 to June 2000

comparisons between winds from VOSs and NSCAT found that the rms differences between NSCAT and VOS wind speeds were roughly three times as large as the differences with our quality-controlled R/V winds (V. Zlotnicki and R. Atlas, 1997, personal communications). Another advantage of ship observations over buoy observations is that the observation height is above the regime where wave motions modify the log-wind profile (Large *et al.,* 1995), which is not the case for buoys in heavy seas. Nevertheless, for most open ocean conditions, there is little difference between the quality of R/V and buoy winds.

The major shortcoming of ship observations is the impact of flow distortion on wind vectors. Directional errors due to flow distortion are reduced by eliminating winds from ship-relative angles that passed through or near the superstructure. Nevertheless, flow distortion does cause wind speed biases. Observational and model-based studies (Yelland *et al.,* 1998; Thiebaux, 1990) applied to different ships indicate that biases due to flow distortion vary from ship to ship. Much of the wind observation record from the R/V Ronald Brown was discarded during our quality control of the ship data (prior to comparison with the scatterometer); most cruises during this time period suffered from severe flow distortion (Chris Fairall, 2000, personal communication). The bias in QuikSCAT, relative to the ships used in this study, ranges from –0.4 to +0.7 ms^{-1}, with most speed biases being within ±0.2 ms^{-1}. One fascinating potential use of high quality scatterometer data is the estimation of biases due to flow distortion. In less than one year of open-ocean operations, there would be sufficient observations (an average of two per day for QuikSCAT) to examine the problem as a function of wind speed and ship-relative wind direction.

Another minor shortcoming of ship data is that one-minute observation intervals are insufficient to remove averaging errors associated with ship acceleration (i.e. changes in speed or direction; Smith *et al.,* 1999). In 1999, the processing of wind data on the R/V Polarstern was changed to calculate true winds every 5 s and average them every minute. The acceleration-related errors are not evident in the winds recorded by this system. Ship winds associated with excessive acceleration are filtered out through the restriction that magnitude of the sum of variance in the component velocities be less than 1.0 $m^2\ s^{-2}$.

3.3 WIND SPEED CALIBRATION

The collocated pairs of winds are also quality controlled to remove gross errors in wind speeds (possibly related to rain) following the criteria of Freilich and Dunbar (1999). Scatterometer winds are compared to ship true winds (Figure 2). The co-location criteria are the closest match within 25 km and usually within 30 seconds. The close fit to the ideal line shows that there is an extremely good match. The apparent bias towards overestimation at low wind speeds is an expected consequence of comparing two quantities that must be positive, each of which has error characteristics expressed as vectors (Freilich, 1997).

3.4 WIND DIRECTION CALIBRATION

Scatterometers are unique among satellite-based wind sensors, in that they determine the wind direction as well as the wind speed. A scatterplot of scatterometer wind direction versus ship wind directions (Figure 3) shows that there is usually a close match. The solid lines indicate an ideal fit, the dotted lines indicate reversed wind directions, and the dashed lines indicate a 90° difference. The tight cluster around the ideal line indicates that in most cases the correct ambiguity is selected. The percentage of correctly selected ambiguities

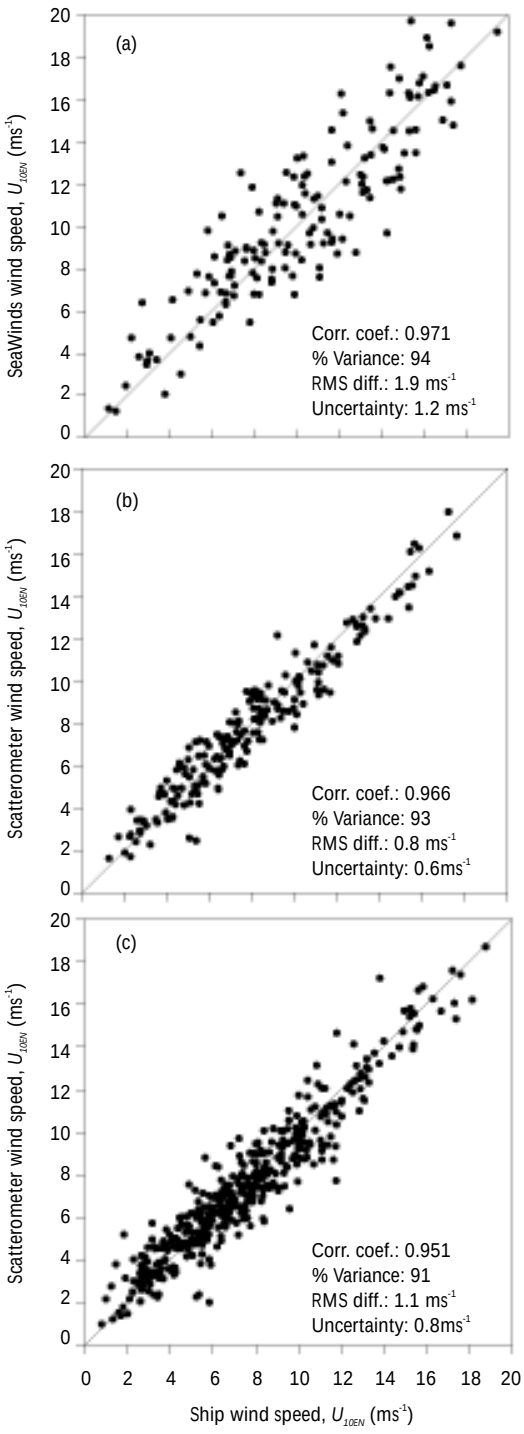

Figure 2—Collocated ship and scatterometer winds: (a) 25 km NSCAT-2; (b) Ku-2000; and (c) QSCAT-1 products. The solid line is the ideal fit. The differences in correlation coefficient and variance explained are related to the accuracy, co-location constraints, and data distribution.

(Figure 4) is 90 per cent for the NSCAT 50 km product and 87 per cent for the 25 km product. QSCAT-1 ambiguity selection skill is 91 per cent, and Ku-2000 skill is 93 per cent. The chance that an incorrect alias is selected is dependent on wind speeds. For $U_{10} > 10$ m s^{-1}, the chance of an incorrect alias is small, except for the (near nadir) QSCAT-1 winds. For $U_{10} < 10$ m s^{-1}, the chance of an incorrect alias increases as the wind speed decreases. QuikSCAT shows a remarkable improvement in low wind speed (<4 m s^{-1}) ambiguity selection, with the percentage of correct selection being almost double that of NSCAT.

3.5 DEPENDENCE OF UNCERTAINTY ON SPATIAL DIFFERENCE IN CO-LOCATION

For QuikSCAT speeds and directions, variance (uncertainty squared) was examined as a function of co-location distance, and a strong dependence on differences in spatial co-location (Figure 5) was found. The rms differences and random uncertainties (one standard deviation) increase as the spatial co-location

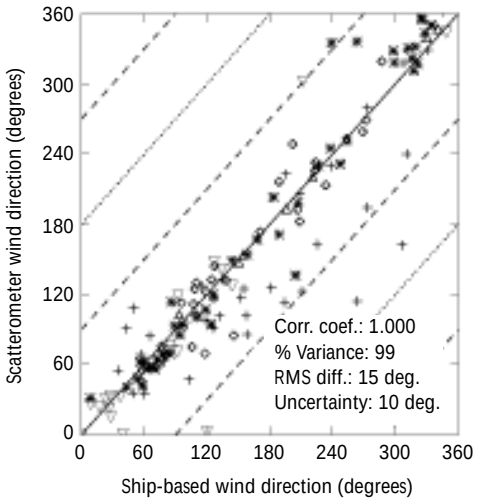

Figure 3—Collocated ship and SeaWinds wind directions. The solid line is the ideal fit, dashed lines are 180° errors, and dotted lines are 90° errors.

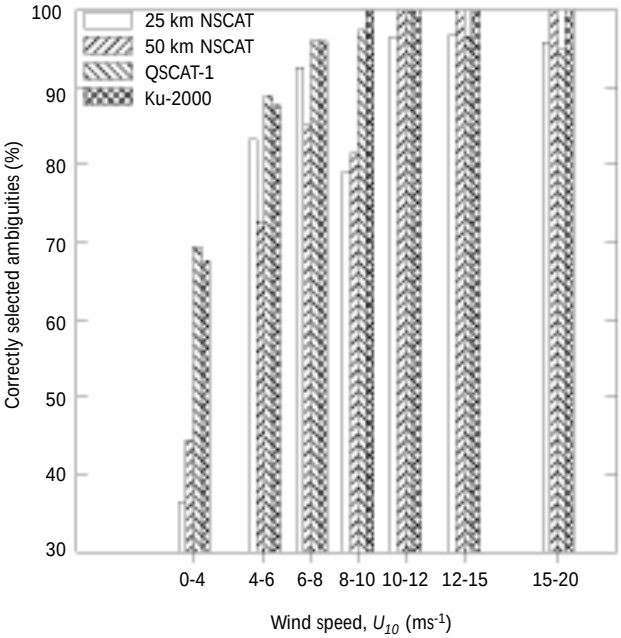

Figure 4—Fraction of correct ambiguity selections for various wind speed bins, for both NSCAT products and SeaWinds on QuikSCAT.

criteria increases. The dependence on spatial differences in co-location can be examined by binning observations in terms of these spatial differences (Figure 5(a)), and then reanalyzing the data in each bin. Variances are determined from the data in each bin, and then extrapolated to zero spatial difference in co-location. The extrapolated variance provides an estimation of observational uncertainty (Bourassa *et al.*, 2001). For co-location distances less than 6 km, the QSCAT-1 uncertainty drops to 0.45 m s^{-1} (0.3 m s^{-1} for Ku-2000; not shown). With this preliminary data set, there is no indication of improvement for smaller co-location distances. Similarly, the variance in direction drops from ~160°^{2} for co-location differences of ~10 km, to ~30°^{2} for co-location differences of ~2 km. Extrapolation with a parabolic best fit estimates an uncertainty of 4°. However, this result is heavily dependent on the point in the 0-2.5 km bin. Additional tests involving the magnitude of vector differences ($|U_{10EN,\ scat} - U_{10EN,\ ship}|$) support an uncertainty of 5° (Bourassa *et al.*, 2001).

3.6 CALIBRATION DEPENDENCE ON WIND SPEED

The accuracy of wind speed and direction for correctly selected ambiguities is not a function of wind speed; however, the accuracy of ambiguity selection is a function of wind speed (Figure 4). Ambiguity selection has little impact (<0.1 ms^{-1}) on wind speed accuracy, but can lead to considerable additional uncertainty in direction. For ERS scatterometers, ambiguity selection is also a function of position in

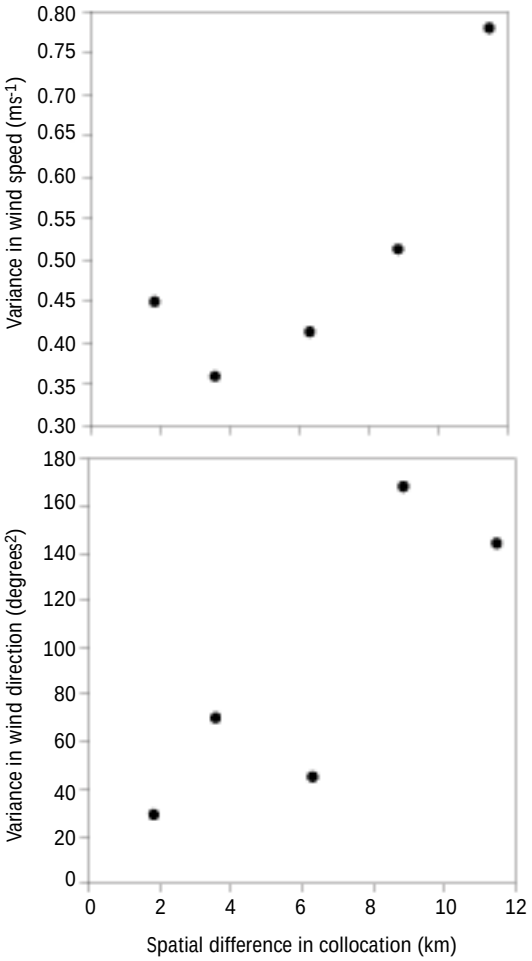

Figure 5—Variance between ship and SeaWinds wind (a) speeds, and (b) directions as functions of co-location distance. Bin size is 2.5 km.

the observational swath (due to shortcomings in the design of the satellite rather than the scatterometer). For other scatterometers, ambiguity selection is largely a problem for low wind speeds. For very low wind speeds (<2 m s^{-1}), these directional uncertainties are easily modelled as random component errors (Freilich, 1997; Freilich and Vanhoff, 2000), and this approach works very well for U_{10} < 8 ms^{-1}. For stronger winds, the random component error model underestimates directional uncertainty (Bourassa *et al.*, 2001). A constant directional uncertainty is a very good model for U_{10} > 8 ms^{-1}, where ambiguity selection is negligible for the NSCAT-2 and Ku-2000 model functions.

4. GRIDDED WIND PRODUCTS

Most oceanographic applications require winds (or stresses) that are on a regular latitude-longitude grid, and that are regular in time. The difficulties in creating such products are twofold: filling the gaps in observations, and the removal of spurious curl and divergence at swath edges and intersections. A large number of regularly gridded scatterometer wind products have become available in the few years since NSCAT winds were validated. For example, Tang and Liu (1996) filled the gaps in daily fields with ECMWF winds, and then applied an objective interpolation. The need for non-scatterometer data was eliminated through interpolation (Polito *et al.*, 1997; IFREMER/CERSAT, 1998; B. Cheng, 1998, personal communication).

Alternatively, wind fields were generated through spatial and/or temporal averages (Bourassa *et al.*, 1998, 1999*b*; Kutsuwada, 1998; Kelley *et al.*, 1999). Usually, these interpolation techniques did not adequately remove the observational pattern, and the averaging or smoothing techniques had too great a reduction in kinetic energy.

An approach designed to remove the observational pattern (Chin *et al.*, 1998) has applied wavelet-based resolution analysis to a combination of NSCAT, ERS-2, and NCEP winds. This approach explicitly preserves wind component energy

spectra seen in longer-term wind field averages (Freilich and Chelton, 1986; Milliff *et al.*, 1999*b*; Wikle *et al.*, 1999). A new approach (Pegion *et al.*, 2000) used a variational method to minimize the misfit to observed pseudostress (the product of scalar and vector winds, which is similar to the surface stress) and minimize the presence of orbital pattern. This approach used cross validation (Wahba and Wendelberger, 1980) to objectively determine the weighting of the constraints used in the variational method. This product has a daily average pseudostress similar to the scatterometer swath winds, and has very little appearance of the observational pattern. The wind component energy spectra are not constrained in this approach; however, these spectra also match the findings of the previous studies. These wind fields clearly show frontogenesis, cyclogenesis, and large-scale wind patterns.

Some caution should be utilized when applying any gridded wind product derived from a polar-orbiting satellite. For example, some gridded products do not adequately deal with the orbital pattern, causing areas with spurious curl and divergence. These spurious features can have considerable negative impact on ocean models. Furthermore, the sampling pattern results in non-uniform error characteristics (Schlax *et al.*, 2000), which can cause features to fluctuate in intensity. Consequently, the accuracy of long-wave or low-frequency signals can be much better than short-wave or high-frequency signals. Local frequency characteristics of the fields can be examined through comparison with buoy winds. For example, the gridded fields of Pegion *et al.* (2000) have been shown to reproduce most of the frequency characteristics of winds from several TAO buoys. Despite these potential problems, scatterometer wind fields are currently the most accurate and highest resolution winds available at this time.

Characteristics of the existing gridded scatterometer products are summarized in Table 5. The listed characteristics are spatial and temporal coverage, and spatial and temporal grid spacing. Links and/or contact information for all the scatterometry products can be found on the COAPS scatterometry web site (http://coaps.fsu.edu/scatterometry/). As new products become available, they will be linked to these web pages.

5. WIND ANIMATIONS

Wind fields (Bourassa *et al.*, 1999*a*; Pegion *et al.*, 2000) were used to produce animations of the winds and vorticity fields. Animations allow the vast quantity of scatterometer data to be easily examined for features of interest. The winds are shown with moving vectors. The motion of the vectors is Lagrangian, and the vector length indicates the wind speed. The changes in vector positions (i.e. motion) are calculated by interpolating the daily wind fields to one hour time steps, and integrating with a fourth order Runge-Kutta method (Kutta, 1901). The Runge-Kutta technique uses an adaptive time step, with a first guess equal to the time interval between frames. This time interval is dependent on the highest wind speeds and tightest circulations; however, a time step of two or three hours was found to be effective for most atmospheric conditions. The animations were designed for easy access. They are available on our web site (http://coaps.fsu.edu/scatterometry/) and are split into weekly animations.

These animations have proven to be extremely useful for visualizing the surface winds. For example, they show previously unsuspected directional variability in winds (Tehuantepecers) flowing from the Gulf of Mexico, through Chevela Pass and into the Gulf of Tehuantepec. These winds typically turn to the right; however, when Hurricane Marco was in the Caribbean Sea, they weakened, turned to the left, and moved through mountain passes in Nicaragua and into the Caribbean Sea (Bourassa *et al.*, 1999*b*). Animations based on the improved fields of Pegion *et al.* (2000) also reveal eddies-associated westerly bursts during the onset of the 1997/98 El Niño.

6. CONCLUSIONS

Quality-controlled and high temporal resolution wind observations from R/Vs have proven to be effective in providing surface comparison data to evaluate the accuracy of scatterometer winds. The SeaWinds design (Ku-band, with large incidence angles) is more sensitive to rain than NSCAT (Ku-band, with smaller

Scatterometer gridded product	*Spatial coverage*	*Spatial grid*	*Temporal coverage*	*Temporal grid*	*Data fields*	*Input data*	*Processing technique*
NSCAT project fast look	Global (in swaths)	0.5 × 0.5°	9/15/96 to 6/29/97	Daily	u, v	NSCAT	Vector average within swaths
QuikSCAT project fast look	Global (in swaths)	0.25 × 0.25°	7/19/99 ongoing	Daily	u, v	QSCAT	Vector average within swaths
Cheng, Chao and Liu	Global	1 × 1°	9/15/96 to 6/29/97	2 Days	u, v	NSCAT, ECMWF	Gaussian-weighted
COAPS/FSU objectively analysed	Indian Ocean 34.5S - 28.5N, 25.5E - 124.5E	1 × 1°	9/15/96 to 6/29/97	Daily	UW, VW	NSCAT	Variational method, with objectively determined weights
	Pacific Ocean 34.5S - 28.5N, 25.5E - 124.5E	1 × 1°	9/15/96 to 6/29/97	Daily	UW, VW	NSCAT	
	Global	1 × 1°	9/15/96 to 6/29/97	Daily	UW, VW	NSCAT	
	Global		07/20/99 ongoing	4×daily		QSCAT	
COAPS/FSU temporal averaged	Global	1 × 1°	9/15/96 to 6/29/97	Daily	u, v	NSCAT	Centered, temporally weighted, mean
COAPS/FSU monthly stresses	Global	0.5 × 0.5°	10/96 to 6/97	Monthly	τ_x, τ_y	NSCAT	Temporal mean
Ifremer/ Cersat	Global	1 × 1°	8/5/91 to 5/1/98	Bi-weekly and Bi-monthly	u, v, τ_x, τ_y, wind div., wind curl	NSCAT and ERS-1/2 Winds	Objective interpolation with a minimum variance method
Kelly, Caruso and Dickinson	Tropical Pacific	1 × 1°	10/1/96 to 6/26/97	Daily	UW, VW	NSCAT	Objective average
Kutsuada	30E to 90W	1 × 1°	9/15/96 to 6/29/97	Daily	yu, v, τ_x, τ_y	NSCAT	Weighted mean vectors
Chin, Milliff and Large	Gobal	0.5 × 0.5°	8/1/96 to 7/31/97	6 hours	u, v	NSCAT, ERS-2, NCEP	Wavelet-based multi-resolution analysis
Polito, Liu and Tang	Global	1 × 1°	9/15/96 to 6/29/97	Daily	u, v τ_x, τ_y, Div. of stress, Ekman pumping	NSCAT	Correlation- based interpolation
Tang and Liu	Global	0.5 × 0.5°	9/15/96 to 6/29/97	12 hours	u, v	NSCAT, ECMWF	Successive correction
		0.25 × 0.25°	9/03/99 ongoing	12 hours	u, v	QSCAT, ECMWF	

Table 5—Regularly gridded products using scatterometer data. The symbols in the data fields column are zonal wind (u), meridional wind (v), wind speed (w), zonal pseudostress (UW), meridional pseudostress (VW), zonal stress (τ_X), and meridional stress (τ_Y). More information on these data sets, including format and access, is available through our web site (http://coaps.fsu.edu/scatterometry/).

incidence angles) or ERS-1/2 (C-band, with smaller incidence angles). Therefore, a rain flag based on QuikSCAT observations is used to remove rain from a set of co-located observations. The uncertainty in the comparison data set and differences in co-location were shown to be essential to the accurate estimate of uncertainty in the satellite winds. Principal component analysis (PCA) was used with co-location differences of less than 12.5 km and 10 minutes to estimate uncertainties for correctly selected ambiguities. The impact of co-location distance was shown by binning variance (uncertainty squared) as a function of co-location distance. Consideration of co-location differences and uncertainty in the comparison data set resulted in uncertainty estimates (for correctly selected ambiguities) of 0.45 m s^{-1} and 5° the SeaWinds QSCAT-1 model function, and 0.3 m s^{-1} and 3° the SeaWinds Ku-2000 model function. The excellent coverage and great accuracy of modern scatterometers will lead to greatly improved wind climatologies, as well as improved wave climatologies based on these winds.

Ambiguity selection was shown to be good for the NSCAT-2 model function (88 per cent), and excellent for SeaWinds observations (91 per cent). For U_{10} >10 m s^{-1}, the chance of an incorrect ambiguity selection is extremely small. Most of the ambiguity selection problems occurred in the $0 < U_{10} < 6$ m s^{-1} range. The greatest difference between NSCAT and SeaWinds ambiguity selection is for $U_{10} < 4$ m s^{-1}, where SeaWinds is almost twice as effective. Many of the ambiguity errors associated with low wind speeds are likely to be associated with uncertainties in both the scatterometer observations and the comparison data set (Freilich, 1997).

The NSCAT and SeaWinds on QuikSCAT winds are more than sufficiently accurate for oceanographic studies on space/time scales greater than 50 km and three days. For regularly gridded products, the winds must be processed in a manner that removes errors related to the observational pattern and retains the observed pseudostress. The gridded products to date (Table 5) have varying degrees of success in meeting these goals. The fully objective technique of Pegion *et al.* (2000) does an excellent job of retaining the observed pseudostress without the appearance of the observational pattern. This consideration is essential for forcing ocean models, as the appearance of the observational pattern is synonymous with spurious wind forcing.

An excellent tool for visualizing the evolution of the wind fields is moving vector animation. The large-scale animations provide a good example of synoptic scale motion and general circulation patterns. The smaller scale animations reveal the larger mesoscale variations. These animations have proven to be useful for finding previously unexpected wind motions and vorticity patterns.

There is a wealth of user-friendly and publicly available scatterometry products. These include swath observations, gridded products, graphics, and animations as well as background information. An updated listing of all these products is available at http://coaps.fsu.edu/scatterometry/.

ACKNOWLEDGEMENTS

We thank the many people who provided observations from the RSV Aurora Australis, R/V Atlantis, R/V Knorr, R/V Melville, R/V Meteor, R/V Oceanus, R/V Polarstern, R/V Ronald Brown, R/V Thompson, and those who quality controlled the observations. The scatterometer data were obtained from the NASA Physical Oceanography Distributed Active Archive Center at the Jet Propulsion Laboratory/California Institute of Technology, and Remote Sensing Systems. Support for the scatterometer research came from the NASA/OSU SeaWinds project and the NASA OVWST project. NSF support of the WOCE DAC/SAC for surface meteorology funded the quality control of research vessel data. COAPS receives its base funding from the Secretary of Navy Grant from ONR to James J. O'Brien.

REFERENCES

Atlas, R., S.C. Bloom, R.N. Hoffman, E. Brin, J. Ardizzone, J. Terry, T.D. Bungato, J.C. Jusem, 1999: Geophysical validation of NSCAT winds using atmospheric data and analyses. *J. Geophys. Res.*, 104, 11,405-11,424.

Bliven, L.F., H. Branger, P.C. Sobieski and J-P. Giovanangeli, 1993: An analysis of scatterometer returns from a water surface agitated by artificial rain. *International Journal of Remote Sensing*, 14, 2315-2329.

Bourassa, M.A., M.H. Freilich, D.M. Legler, W.T. Liu and J.J. O'Brien, 1997: Wind observations from new satellite and research vessels agree. EOS Trans. of *Amer. Geophys. Union*, 78, 597 & 602.

Bourassa, M.A., D.G. Vincent and W.L. Wood, 1999*a*: A flux parameterization including the effects of capillary waves and sea state. *J. Atmos. Sci.*, 56, 1123–1139.

Bourassa, M.A., L. Zamudio and J.J. O'Brien, 1999*b*: Non-inertial flow in NSCAT observations of Tehuantepec winds. *J. Geophys. Res.*, 104, 11,311–11,320.

Bourassa, M.A., D.M. Legler, J.J. O'Brien and S.R. Smith, 2001: SeaWinds validation with research vessels, *J. Geophys. Res.*, submitted.

Bourassa, M.A., D.M. Legler, J.J. O'Brien, J.N. Stricherz and J. Whalley, 1998: High temporal and spatial resolution animations of winds observed with the NASA scatterometer, 14th International conference on IIPS (January, Phoenix, AZ), American Meteorological Society, 556–559.

Cardone, V.J. (1969): Specification of the wind distribution in the marine boundary layer for wave forecasting. Geophys. Sci. Lab. N.Y. *Univ. Report TR-69-1* (NTIS AD 702-490).

Cardone, V.J., R.E. Jensen, D.T. Resio, V.R. Swail and A.T. Cox, 1996: Evaluation of contemporary ocean wave models in rare extreme events: The "Halloween Storm" of October 1991 and the "Storm of the Century" of March 1993. *J. Atmos. Oceanic Technol.*, 13, 198-230.

Caruso, M.J., K.A. Kelly, M. McPhaden and S. Dickinson, 1997: Evaluation of scatterometer winds using Equatorial Pacific buoy observations. *Proceedings of the NASA Scatterometer Symposium* (10-14 November 1997 Maui, Hawaii) [Available from the Scatterometer Projects Office, Jet Propulsion Lab., Pasadena, California].

Caruso, M.J., S. Dickinson, K.A. Kelly, M. Spillane, L.J. Mangum, M. McPhaden and L.D. Stratton, 1999: Evaluation of NSCAT scatterometer winds using Equatorial Pacific buoy observations. *WHOI Technical Report 99-10* [Available from Woods Hole Oceanographic Institution, Woods Hole, Massachusetts 02543, USA].

Chelton, D.B. and F.J. Wentz, 1986: Further development of an improved altimeter wind speed algorithm, *J. Geophys. Res.*, 91, 14250-14260.

Chelton, D.B., M.H. Freilich and S.K. Esbensen, 2000: Satellite observations of the wind jets off Central America, Part II: Regional relationships and dynamical considerations. *Mon. Wea. Rev.*, 128, 1993-2018.

Chin, T.M., R.F. Milliff and W.G. Large, 1998: Basin scale, high-wavenumber sea surface wind fields from a multi-resolution analysis of scatterometer data. *J. Atmos. Ocec. Tech.*, 15, 741-763.

Dickenson, S., K.A. Kelly, M.J. Caruso and M.J. McPhaden, 2000: A note on comparisons between the TAO buoy and NASA scatterometer wind vectors. *J. Atmos. Ocec. Tech.*, accepted.

Ebuchi, N., 1999: Statistical distribution of wind speeds and directions globally observed by NSCAT. *J. Geophys. Res.*, 104, 11393-11404.

Freilich, M.H., 1997: Validation of vector magnitude data sets: effects of random component errors. *J. Atmos. Oceanic Technol.*, 14, 695-703.

Freilich, M.H. and D.B. Chelton, 1986: Wavenumber spectra of Pacific winds measured by the SeaSat scatterometer. *J. Phys. Oceanogr.*, 16, 741-757, 1986.

Freilich, M.H. and R.S. Dunbar, 1999: The accuracy of the NSCAT 1 vector winds: Comparison with National Data Buoy Center buoys. *J. Geophys. Res.* 104, 11231-11246.

Freilich M.H. and B.A. Vanhoff, 2000: The accuracy of remotely sensed surface wind speed measurements. *J. Atmos. Oceanic Technol.*, in review.

Gonzales, A.E. and D.G. Long, 1999: An assessment of NSCAT ambiguity removal. *J. Geophys. Res.*, 104, 11449-11458.

Graber, H.C., N. Ebuchi, R. Vakkayil, 1996: Evaluation of ERS-1 scatterometer winds with wind and wave ocean buoy observations. *RSMAS Technical Report* 96-003 [available from the Rosenstiel School of Marine and Atmospheric Science, University of Miami, Miami, FL 33149-1098, USA].

Graber, H.C., A. Bentamy and N. Ebuchi, 1997: Evaluation of scatterometer winds with ocean buoy observations. *Proceedings of the NASA Scatterometer Symposium* (10-14 November 1997, Maui, Hawaii) [available from the Scatterometer Projects Office, Jet Propulsion Lab., Pasadena, California].

IFREMER/CERSAT, 1998: Mean surface wind fields from the ERS-AMI and ADEOS-NSCAT microwave scatterometers, 91/08/05 to 98/03/01. A contribution to WOCE, a CD-ROM published for the WOCE conference (Halifax, Canada).

Jones, W.L., V.J. Cardone, WJ. Pierson, J. Zec, L.P. Rice, A. Cox and W.B. Sylvester, 1999: NSCAT high-resolution surface wind measurements in Typhoon Violet. *J. Geophys. Res.*, 104, 11247-11260.

Katsaros, K.B. and R.A. Brown, 1991: Legacy of SeaSat mission for studies of the atmosphere and air-sea-ice interactions. *Bull. Amer. Meteor. Soc.*, 72, 967-981.

Kelly, K.A., S. Dickinson and Z.-J. Yu, 1999: NSCAT Tropical wind stress maps: Implications for improving ocean modeling. *J. Geophys. Res.*, 104, 11291-11310.

Kutta, W. 1901: Beitrag zur näherungsweisen integration totaler differentialgleichungen. *Z Math. Phys.* 46, 435-453.

Kutsuwada, K., 1998: Impact of wind/wind-stress field in the North Pacific constructed by ADEOS/NSCAT data., *J. Oceanogr.*, 54, 443-456.

Large, W.G., J. Morzel and G.B. Crawford, 1995: Accounting for surface wave distortion of the marine wind profile in low-level ocean storm wind measurements, *J. Phys. Oceanogr.*, 25, 2959 - 2971.

Liu, W.T. and W. Tang, 1996: Equivalent Neutral Wind, *JPL Publication* 96-17, Jet Propulsion Laboratory, California Institute of Technology, CA.

Milliff, R.F., T.J. Hoar, H. van Loon and M. Rapheal, 1999*a*: Quasi-stationary wave variability in NSCAT winds. *J. Geophys. Res.,* 104, 11,425–11,436.

Milliff, R.F., W.G. Large, J. Morzel, G. Danabasoglu and T.M. Chin, 1999*b*: Ocean general circulation model sensitivity to forcing from scatterometer winds. *J. Geophys. Res.*, 104, 11,337-11,358.

Moore, R.K., D. Chatterjee and S. Taherion, 1999: Algorithm for correcting SeaWinds/ADEOS-II for rain attenuation. *Proceedings of the QuikSCAT Cal/Val – Early Science Meeting* (Arcadia, CA.) [Available from Scatterometer Projects Office, Jet Propulsion Lab., Pasadena, CA 91109].

Naderi, F.M., M.H. Freilich and D.G. Long, 1991: Spaceborne radar measurements of wind velocity over the ocean — an overview of the NSCAT scatterometer system. *Proceedings of the IEEE*, 79, 850-866.

Pearson, K., 1901: On lines and planes of closest fit to systems of points in space. *Phil. Mag.*, 2, 59-572.

Pegion, P.J., M.A. Bourassa, D.M. Legler and J.J. O'Brien, 2000: Objectively derived daily pseudostress fields from NSCAT data created through direct-minimization, cross validation, and multigridding. *Mon. Wea. Rev.*, 128, 3150–3168.

Pierson, W.J., Jr, 1990: Examples of, reasons for and consequences of the poor quality of wind data from ships for the marine boundary layer: implications for remote sensing, *J. Geophys. Res.*, 13,313 - 13,340.

Polito, P.S., W.T. Liu and W. Tang, 1997: Correlation-based interpolation of NSCAT wind data. NSCAT Science Working Team Meeting (Maui, Hawaii, November, 1997).

Preisendorfer, R.W. and C.D. Mobley, 1988: *Algebraic Foundations of PCA, Principal Component Analysis in Meteorology and Oceanography*. Elsevier, 11 - 24.

Ross, D.B., V.J. Cardone, J. Overland, R.D. McPherson, W.J. Pierson Jr. and T. Yu, 1985: Oceanic surface winds. *Adv. Geophys.*, 27, 101-138.

Schlax, M.G., D.B. Chelton and M.H. Freilich, 2000: The effects of sampling errors in wind fields constructed from single and tandem scatterometer datasets. *J. Atmos. Oceanic Technol.*, submitted.

Smith, S.R., M.A. Bourassa and R.J. Sharp, 1999: True winds from vessels at sea: Requirements and implications for automated maritime observing systems, *J. Atmos. Oceanic Technol.*, 16, 939–952.

Sobieski, P.W, C. Craeye and L.F Bliven, 1999: Scatterometric signatures of multivariate drop impacts on fresh and salt water surfaces. *International Journal of Remote Sensing*, 20: 2149-2166.

Sobieski, P. and L.F. Bliven, 1995: Analysis of high speed images of raindrop splash products and ku-band scatterometer returns. *International Journal of Remote Sensing*, 16, 2721-2726.

Stoffelen A., 1998: Toward the true near-surface wind speed: Error modeling and calibration using triple collocation. *J. Geophys. Res.*, 103, 7755 - 7766.

Tang, W. and W.T. Liu, 1996: *Objective Interpolation of Scatterometer Winds.* Technical Report 96-19, Jet Propulsion Laboratory, California Institute of Technology, CA.

Thiebaux, M.L., 1990: Wind tunnel experiments to determine correction functions for shipborne anemometers. *Canadian Contractor Rep. Hydrog. & Ocean Sci.* 36, BIO, Dartmouth, Nova Scotia, 57 pp.

Verschell, M.A., M.A. Bourassa, D.E. Weissman and J.J. O'Brien, 1999: Model validation of the NASA scatterometer winds, *J. Geophys. Res.*, 104, 11,359–11,374.

Wahba, G. and J. Wendelberger, 1980: Some new mathematical methods for variational objective analysis using splines and cross-validation. *Mon. Wea. Rev.*, 108, 1122-1143.

Weissman, D.E., M.A. Bourassa and J. Tongue, 2000: Effects of rain-rate and wind magnitude on SeaWinds scatterometer wind speed errors. *J. Atmos. Oceanic Technol.*, submitted.

Wentz, F.J. and D.K. Smith, 1999: A model function for the ocean-normalized radar cross section at 14 GHz derived from NSCAT observations. *J. Geophys. Res.*, 104, 11499-11514.

Wikle, C.K., R.F. Millif and W.G. Large, 1999: Surface wind variability on spatial scales from 1 to 1000 km observed during TOGA COARE. *J. Atmos. Sci.*, 56, 2222-2231.

Yelland, M.J., B.I. Moat, P.K. Taylor, R.W. Pascal, J. Hutchings and V.C. Cornell, 1998: Wind stress measurements from the open ocean corrected for airflow distortion by the ship. *J. Phys. Oceanogr.*, 28, 1511–1526.

Zeccheto, S, I. Tanduo and Y. Quilfen, 1999: The CERSAT dealiasing of ERS-2 scatterometer winds in the Mediterranean Sea. *CERSAT NEWS*, Scientific Topic number 2, 1-4.